Contents lists available at ScienceDirect

Solid State Communications

Temperature dependence of the pressure induced monoclinic distortion in the spin $S = 1/2$ Shastry–Sutherland compound SrCu$_2$(BO$_3$)$_2$

M.E. Zayed [a,b,c,*], Ch. Rüegg [c,d,e], E. Pomjakushina [f], M. Stingaciu [f,g], K. Conder [f], M. Hanfland [h], M. Merlini [h], H.M. Rønnow [b]

[a] Department of Mathematics, Statistics and Physics, College of Arts and Science, Qatar University, P.O. Box 2713, Doha, Qatar
[b] Laboratory for Quantum Magnetism, Ecole Polytechnique Federal de Lausanne (EPFL), 1015 Lausanne, Switzerland
[c] Laboratory for Neutron Scattering, Paul Scherrer Institute, 5232 Villigen PSI, Switzerland
[d] London Centre for Nanotechnology and Department of Physics and Astronomy, University College London, London WC1E 6BT, UK
[e] Department of Condensed Matter Physics, University of Geneva, 1211 Geneva, Switzerland
[f] Laboratory for Developments and Methods, Paul Scherrer Institute, 5232 Villigen PSI, Switzerland
[g] Department of Materials and Environmental Chemistry, Stockholm University, Stockholm S-106 91, Sweden
[h] ESRF, F-38043 Grenoble Cedex, France

ARTICLE INFO

ABSTRACT

We investigate the monoclinic distortion that occurs at 4.7 GPa at room temperature in the frustrated Shastry–Sutherland model quantum magnet SrCu$_2$(BO$_3$)$_2$ as a function of pressure and temperature by means of powder and single crystal angle dispersive synchrotron X-ray diffraction. Our results indicate that the onset of the structural distortion varies in a narrow pressure range between $\sim$4.0 and 5.0 GPa. This result will be useful in order to distinguish between magnetic transitions related to structural changes and potential intrinsic quantum phase transitions that various reports have suggested to take place in SrCu$_2$(BO$_3$)$_2$ at high pressure and low temperature.

1. Introduction

The compound SrCu$_2$(BO$_3$)$_2$ [1,2] is a quasi two-dimensional quantum magnet where the $S = 1/2$ spins of Cu^{2+} ions realize the Shastry–Sutherland model [3]. Frustration of the next nearest neighbor couplings enables a singlet ground state to prevail within a large range of the phase diagram of the Shastry–Sutherland model. SrCu$_2$(BO$_3$)$_2$ has attracted considerable interest in the field of frustrated magnetism for its remarkable properties such as dispersionless triplet excitations [4], magnetization plateaus [5–7], as well as possible formation of exotic ground states [8–10], superconducting [11–13], superfluid and supersolid phases [14,15].

At ambient conditions, SrCu$_2$(BO$_3$)$_2$ crystallizes in the tetragonal non-centro-symmetric space group I$\bar{4}$2 m with lattice parameters $a = b = 8.99$ Å, $c = 6.45$ Å [1]. Each Cu^{2+} ion is connected to its unique nearest neighbor Cu^{2+} ion by two oxygens atoms (exchange J_1) and to its four next nearest neighbors by planar BO$_3$ groups (exchange J_2).

The magnetic CuBO$_3$ planes are well isolated from each other by intercalated Sr layers.

The coupling parameter ratio J_2/J_1 of this compound places it close to a predicted quantum phase transition to other phases with long range order or more complex symmetries. The nature of these phases has been widely debated (see Ref. [16] for a review). Pressure is a tool of choice to tune magnetic couplings and thereby enables to explore the Shastry–Sutherland phase diagram for which SrCu$_2$(BO$_3$)$_2$ is the only known spin $S = 1/2$ realization. Previous studies [17–20] have indicated that pressure actually drives the compound even closer to a magnetic quantum phase transition.

Pressure, however, can also cause structural transitions, and a tetragonal to monoclinic distortion in SrCu$_2$(BO$_3$)$_2$ was indeed discovered by Loa et al. [21] at 4.7 GPa at room temperature. The compression of the a- and b-axis, defining the magnetic 2D plane, is found to be much less pronounced than that of the c-axis, which is consistent with the layered structure of the material. On the other hand, at low temperature and ambient pressure, SrCu$_2$(BO$_3$)$_2$ remains in the I$\bar{4}$2 m tetragonal space group. Strong magneto-elastic effects are observed upon entering the spin-gap regime ($T \sim 35$ K) [22]. These magneto-elastic effects have been used in

* Corresponding author at: Department of Mathematics, Statistics and Physics, College of Arts and Science, Qatar University, P.O. Box 2713, Doha, Qatar. Tel.: +974 662318 36.
E-mail address: mohamed.zayed@qu.edu.qa (M.E. Zayed).

combined pressure and temperature dependent X-ray diffraction measurements to detect signs of quantum phase transitions [20]. There, a change in the compressibility of the *a*-axis was recorded around 4.5 GPa at 4 K. Applying an additional external magnetic field of 7 T magnetic ordering has been reported below 4 K at 2.4 GPa by NMR measurements [18].

Magnetic ordering could occur both from a structural distortion relieving the next nearest neighbor frustration and from the tuning, within the original frustrated Shastry–Sutherland lattice, of the couplings beyond a critical J_2/J_1 ratio estimated to be around 0.9 [16]. The purpose of this study is thus the determination of the structural phase boundaries as a function of pressure and temperature, which is essential in order to distinguish between those two scenarios.

2. Experimental

Angle dispersive synchrotron X-ray diffraction measurements were performed at the high-pressure beam line ID9a of the European Synchrotron Research Facility (ESRF, Grenoble). The wave length was set to $\lambda = 0.4148$ Å and data were recorded on a MAR555 flat panel detector. Powder diffraction data were integrated azimuthally using the FIT2D software [23]. Pressure was generated by a diamond anvil cell (DAC) and ranged from ambient to 19 GPa. Helium was used as a pressure transmitting medium. The pressure was measured by the ruby luminescence method [24]. The uncertainty related to the ruby calibration curve can be estimated to about 0.02 GPa for a pressure of 4.50 GPa [25,26]. Temperature was varied between ambient and 25 K with a helium cooled cryostat. Two types of samples where used :

1. $SrCu_2(BO_3)_2$ powder samples synthesized by solid state reaction with a method similar to Ref. [27]. The powder contains small fractions of impurity phases identified as CuO and Sr (B_2O_4). The DAC is typically rotated by $\pm 3°$ during exposition.
2. $SrCu_2(BO_3)_2$ high quality single crystals of approx. $30 \times 30 \times 5\ \mu m^3$ obtained from fragments of several centimeters long single crystalline rod grown by the traveling solvent floating zone technique with a method similar to Ref. [28]. The single crystals are naturally cleaved along the $a-b$ plane. The DAC is typically rotated by $\pm 10°$ during exposition with the central position corresponding to the *c-axis* parallel to the X-ray beam.

3. Results and discussion

3.1. Powder diffraction

At 202 K powder diffraction patterns were collected in fine steps (34 pressures between 2.0 and 7.5 GPa) upon pressure increase. Temperature was then cycled from 200 K to 30 K with pressure increase between each cycle. This resulted in 6–10 pressure values for each temperature studied, containing 1–6 pressures in the high pressure monoclinic phase. The impurities in the powder sample did not allow for a full refinement of the crystal structure under pressure. We thus followed the splitting of the (2,1,1) Bragg peak as a function of pressure (Fig. 1), marking the tetragonal to monoclinic transition. This peak with its high multiplicity is one of the most sensitive indicators for the phase transition that we could observe in the diffraction patterns. It has a multiplicity 16 in the tetragonal phase and splits into 4 non-equivalent branches upon entering the monoclinic phase. Each of those can be assumed to have the maximal multiplicity 4 of the monoclinic Laue class 2/m. At 202 K, the splitting starts to become visible around 4.3 GPa and is fully resolved by our instrumental resolution above 5.0 GPa.
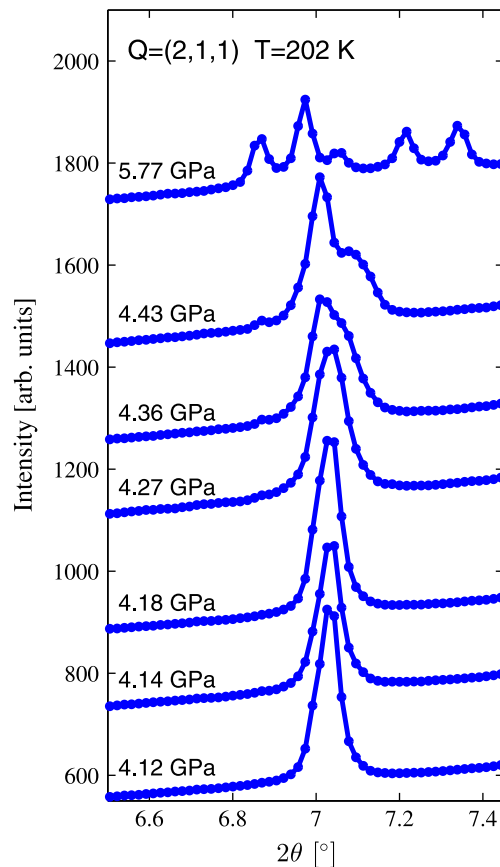

Fig. 1. (Color online) Pressure dependence of the (2,1,1) Bragg reflection in a $SrCu_2(BO_3)_2$ powder sample at $T = 202$ K. The tetragonal reflection splits into non-equivalent monoclinic reflections. The small central peak at the highest pressure originates from an impurity. Data is shifted vertically for clarity.

The Bragg peaks are fitted by Gaussians in order to determine their center positions and widths. The center positions of the split peaks are simultaneously fitted (Fig. 2) to a power law function $f(p) = \delta a_i |p - p_c|^\varepsilon + b + s(p - p_c)$, where the a_i ($i = 1$–4) are the amplitudes of the split for each branch, p_c the critical pressure, b the peak position at p_c, s a linear slope, ε the exponent of the power law and δ is 0 if $p \leq p_c$ and 1 otherwise. In order to account for the possibility that split peaks are not resolved by our instrumental resolution, we use the width of the Bragg peak as error bar for the center position instead of the statistical error on the peak centers which is very small.

For the datasets at lower temperature, the exponent is fixed to $\varepsilon = 0.42 \pm 0.01$ obtained from the fine stepped 202 K data (Fig. 2a). With the exponent fixed, its possible to fit datasets containing only one high pressure point in the monoclinic region. The uncertainty on p_c is essentially determined by the uncertainty on the exponent and reaches a maximum of ± 0.3 GPa in our datasets. The results of the fits are shown for temperatures between 180 and 30 K in Fig. 2b–h.

Fig. 3 shows the critical pressure extracted from one of the cooling cycles where pressure and temperature simultaneously reduced from 5.8 GPa, 180 K to 3.8 GPa, 25 K. The procedure to extract p_c is similar to the one described above, with no fixed parameter in the power law fit. p_c is found to be 4.47 GPa, for a critical temperature of 121 K. This is in acceptable agreement with the value 4.6 ± 0.1 GPa obtained on the 121 K isotherm.

3.2. Single crystal diffraction

The results from the powder sample are complemented by single crystal measurements at 300 K, 105 K and 29 K. At 105 K (Fig. 4),
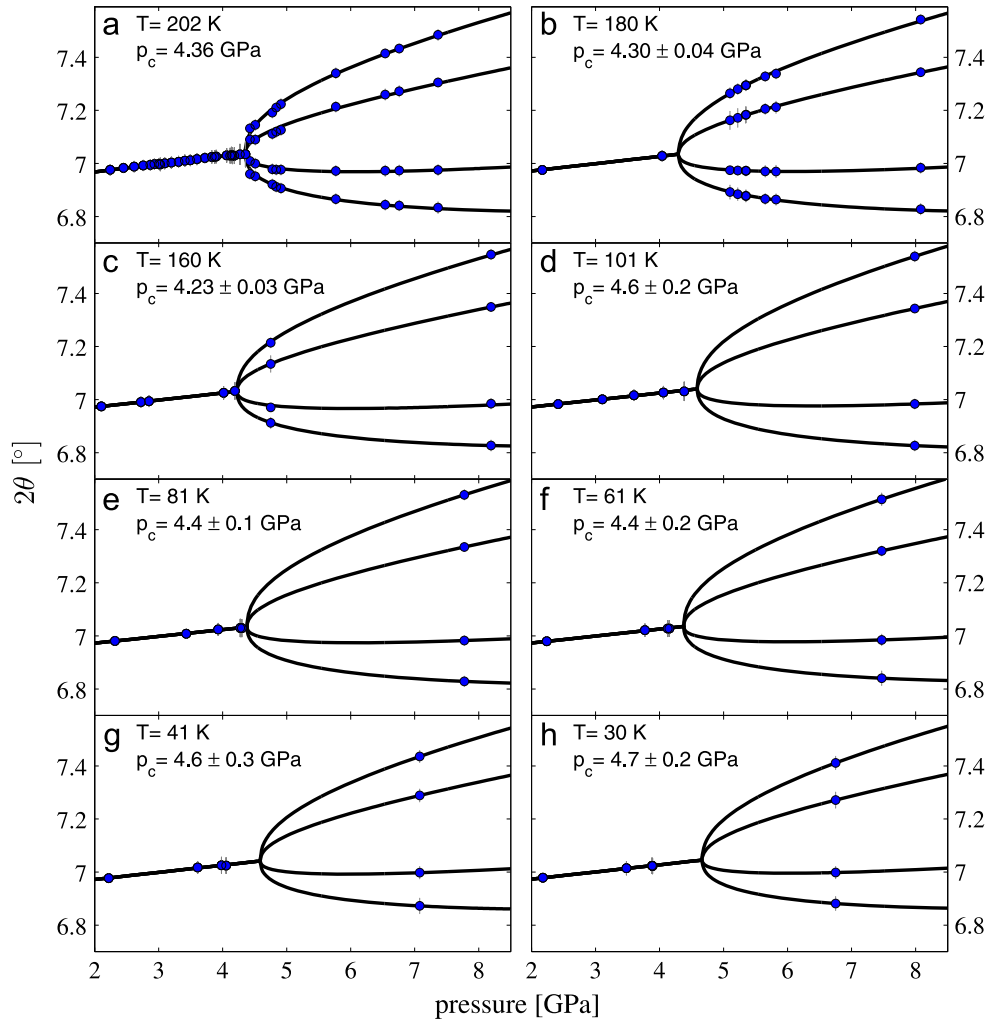
Fig. 2. (Color online) Fits to a power law of the splitting of the (2,1,1) reflection at different temperatures in a powder sample. The fitting procedure is described in the text. The error bars displayed do *not* correspond to the statistical error on the peak centers (those are smaller than the symbols) but represent the *width* of the Bragg peaks. The statistical fit uncertainty for p_c at 202 K is much smaller than the 0.02 GPa uncertainty from the calibration of the pressure scale.
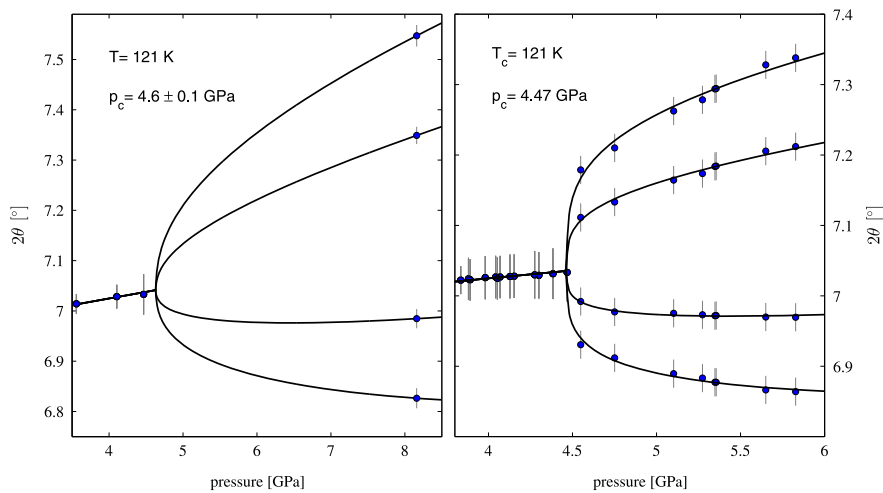

Fig. 3. (Color online) Fits to a power law of the splitting of the (2,1,1) reflection in a powder sample. *Left*: data collected on the 121 K isotherm similar to Fig. 2. *Right*: data collected upon cooling down the sample from 180 K to 25 K through the phase transition with simultaneous pressure reduction from 5.8 GPa to 3.8 GPa. The transition is observed at 121 K and 4.47 GPa. The fitting procedure is described in the text.

14 diffraction patterns were collected upon increasing pressure from 4.0 to 8.0 GPa. We analyze the splitting of the (5,1,0) Bragg peak with a procedure similar to the one used for the powder data with

free parameters in the power law fit (Fig. 5). This peak is observed to have a sudden change in position above 4.59 GPa. It then broadens indicating an underlying double peak structure, that is eventually
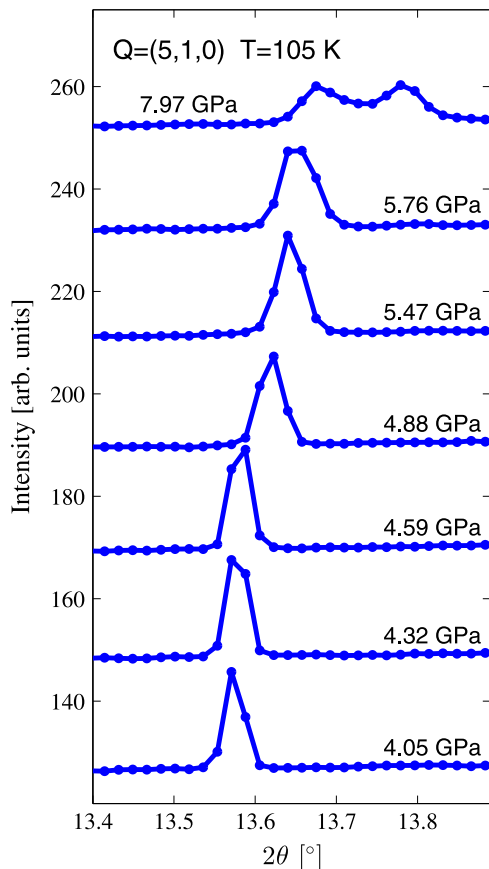
Fig. 4. (Color online) Pressure dependence of the (5,1,0) Bragg reflection in a SrCu$_2$(BO$_3$)$_2$ single crystal sample at $T=105$ K. The tetragonal reflection splits into two equivalent monoclinic reflections. Data is shifted vertically for clarity.
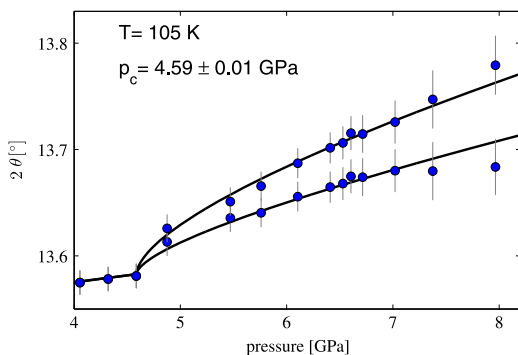

Fig. 5. (Color online) Fits to a power law of the splitting of the (5,1,0) reflection in a single crystal sample. The fitting procedure is described in the text.

resolved with our instrumental resolution around 8.0 GPa. This is in agreement with a monoclinic distortion: upon entering the mono-clinic phase, the β lattice angle is modified which produces the change in the scattering angle 2θ. The β angle itself is pressure dependent [21], and it can be observed that 2θ becomes more pressure dependent in the new phase, as compared to the tetragonal phase where it is determined only by the hard a- and b-axis for a peak with Miller index $L=0$ as (5,1,0). In terms of multiplicity, the data is consistent with the original tetragonal multiplicity 8 leading to 2 distinct monoclinic peaks each with the maximal multiplicity 4. The lower multiplicity and $L=0$ index in (5,1,0) explain the higher pressure needed to resolve the splitting as compared to the (2,1,1) from the powder sample. The critical pressures obtained for the single crystal data are compatible with the powder analysis. At 300 K,
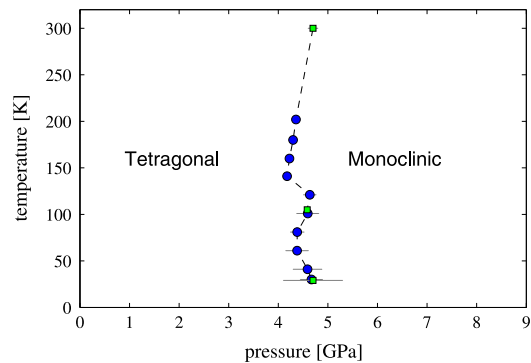

Fig. 6. (Color online) Phase boundary for the monoclinic distortion as function of pressure and temperature. The symbols with horizontal error bars give the critical (p,T) determined by X-ray diffraction and they are connected by the dashed line. Circles are obtained from powder diffraction and squares from single crystal diffraction data.

a similar procedure gives the same critical pressure 4.7 ± 0.1 GPa as in Ref. [21]. Finally the single crystal measurements at 29 K show a tetragonal pattern at 4.1 GPa while a monoclinic pattern is observed at 5.3 GPa. This confirms the powder data analysis and leads to a critical pressure of 4.7 ± 0.6 GPa, where the uncertainty is conservatively chosen as the full range between the two pressures measured.

3.3. Phase diagram

Fig. 6 shows the obtained boundary between the tetragonal and the monoclinic phases determined by the analysis detailed above. Critical points from powder (circles) and single crystal (squares) samples show a good agreement. Considering the general shape of the phase boundary, we observe that, over the entire temperature range, the critical pressure remains essentially between 4.0 and 5.0 GPa. It can be noticed that, upon cooling from ambient, the boundary first curves in towards lower pressures reaching a minimum of about 4.2 GPa at 140 K. It then bends out to slightly higher pressures at 121 K. The tendency at low temperature is more difficult to ascertain given the size of the error bars. It is highly unlikely, however, that the transition occurs below 4.0 GPa or above 5.0 GPa for any temperature.

4. Conclusion

In summary we have tracked the tetragonal to monoclinic structural distortion in SrCu$_2$(BO$_3$)$_2$ as a function of pressure and temperature, by means of synchrotron X-ray single crystal and powder diffraction. The transition between both phases occurs in a narrow pressure range between 4.0 GPa and 5.0 GPa. This result enables to distinguish between intrinsic quantum phase transitions and structurally driven magnetic ordering that are expected to take place in SrCu$_2$(BO$_3$)$_2$ at high pressure. We therefore conclude that potential magnetic pressure induced phase transitions reported below 4.0 GPa are intrinsic and not caused by the structural distortion.

Acknowledgment

References

[1] R.W. Smith, D.A. Keszle, J. Solid State Chem. 93 (2) (1991) 430.
[2] H. Kageyama, K. Yoshimura, R. Stern, N. Mushnikov, K. Onizuka, M. Kato, K. Kosuge, C. Slichter, T. Goto, Y. Ueda, Phys. Rev. Lett. 82 (15) (1999) 3168.
[3] B.S. Shastry, B. Sutherland, Physica B 108 (1–3) (1981) 1069.
[4] H. Kageyama, M. Nishi, N. Aso, K. Onizuka, T. Yosihama, K. Nukui, K. Kodama, K. Kakurai, Y. Ueda, Phys. Rev. Lett. 84 (25) (2000) 5876.
[5] K. Kodama, J. Yamazaki, M. Takigawa, H. Kageyama, K. Onizuka, Y. Ueda, J. Phys.: Condens. Matter 14 (17) (2002) L319.
[6] G. Jorge, R. Stern, M. Jaime, N. Harrison, J. Bonea, S. El Shawish, C.D. Batista, H.A. Dabkowska, B.D. Gaulin, Phys. Rev. B 71 (2005) 092403.
[7] J. Dorier, K.P. Schmidt, F. Mila, Phys. Rev. Lett. 101 (2008) 250402.
[8] A. Koga, N. Kawakami, Phys. Rev. Lett. 84 (19) (2000) 4461.
[9] A. Läuchli, S. Wessel, M. Sigrist, Phys. Rev. B 66 (1) (2002) 014401.
[10] Z. Weihong, J. Oitmaa, C.J. Hamer, Phys. Rev. B 65 (1) (2002) 014408.
[11] B.S. Shastry, B. Kumar, Prog. Theor. Phys. Suppl. 145 (2002).
[12] T. Kimura, K. Kuroki, R. Arita, H. Aoki, Phys. Rev. B 69 (2004) 054501.
[13] B.J. Yang, Y.B. Kim, J. Yu, K. Park, Phys. Rev. B 77 (2008) 104507.
[14] T. Momoi, K. Totsuka, Phys. Rev. B 61 (5) (2000) 3231.
[15] K. Schmidt, J. Dorier, A. Läuchli, F. Mila, Phys. Rev. Lett. 100 (2008) 090401.
[16] S. Miyahara, K. Ueda, J. Phys.: Condens. Matter 15 (2003) 327.
[17] H. Kageyama, N.V. Mushnikov, M. Yamada, Y.U. T Goto, Physica B 329–333 (2003) 1020.
[18] T. Waki, Karai, M. Takigawa, Y. Saiga, Y. Uwatoko, H. Kageyama, Y. Ueda, J. Phys. Soc. Jpn. 76 (2007) 073710.
[19] T. Sakurai, M. Tomoo, S. Okubo, H. Ohta, K. Kudo, Y. Koike, J. Phys.: Conf. Ser. 150 (2009) 042171.
[20] S. Haravifard, A. Banerjee, J. Land, G. Srajer, D. Silevitch, B. Gaulin, H. Dabkowska, T. Rosenbaum, Proc. Natl. Acad. Sci. USA 109 (7) (2011) 2286.
[21] I. Loa, F.X. Zhang, K. Syassen, P. Lemmens, W. Crichton, H. Kageyama, Y. Ueda, Physica B 359–361 (2005) 980.
[22] C. Vecchini, O. Adamopoulos, L.C. Chapon, A. Lappas, H. Kageyama, Y. Ueda, F. Zorko, J. Solid State Chem. 182 (2009) 3275.
[23] A. Hammersley, S. Svensson, M. Hanfland, A. Fitch, D. Hausermann, High Press. Res. 14 (1996) 235.
[24] H.K. Mao, J. Xu, P.M. Bell, J. Geophys. Res. 92 (1986) 4673.
[25] A.D. Chijioke, W.J. Nellis, A. Soldatov, I.F. Silvera, J. Appl. Phys. 98 (2005) 114905.
[26] K. Nakano, Y. Akaham, Y. Ohishi, H. Kawamura, Jpn. J. Appl. Phys. 39 (2000) 1249.
[27] H. Kageyama, K. Onizuka, T. Yamauchi, Y. Ueda, J. Cryst. Growth 206 (1999) 65.
[28] B.D. Gaulin, S.H. Lee, S. Haravifard, J.P. Castellan, A.J. Berlinsky, H.A. Dabkowska, Y. Qiu, J.R.D. Copley, Phys. Rev. Lett. 93 (26) (2004) 267202.